Biochemical and Biophysical Research Communications 594 (2022) 57–62

Contents lists available at ScienceDirect

Biochemical and Biophysical Research Communications

journal homepage: www.elsevier.com/locate/ybbrc

Quantification of single-strand DNA lesions caused by the topoisomerase II poison etoposide using single DNA molecule imaging

Vandana Singh [a, b, **], Pegah Johansson [b, c], Elina Ekedahl [a], Yii-Lih Lin [a], Ola Hammarsten [b, c], Fredrik Westerlund [a, *]

[a] Biology and Biological Engineering, Chalmers University of Technology, Gothenburg, Sweden
[b] Laboratory of Clinical Chemistry, Sahlgrenska University Hospital, Gothenburg, Sweden
[c] Department of Laboratory Medicine, Institute of Biomedicine, Sahlgrenska Academy at University of Gothenburg, Gothenburg, Sweden

ARTICLE INFO

Article history:
Received 15 November 2021
Accepted 11 January 2022
Available online 15 January 2022

Keywords:
Single molecule imaging
DNA damage
Nick translation
Chemotherapy
Single-strand breaks
Base excision repair

ABSTRACT

DNA-damaging agents, such as radiation and chemotherapy, are common in cancer treatment, but the dosing has proven to be challenging, leading to severe side effects in some patients. Hence, to be able to personalize DNA-damaging chemotherapy, it is important to develop fast and reliable methods to measure the resulting DNA damage in patient cells. Here, we demonstrate how single DNA molecule imaging using fluorescence microscopy can quantify DNA-damage caused by the topoisomerase II (TopoII) poison etoposide. The assay uses an enzyme cocktail consisting of base excision repair (BER) enzymes to repair the DNA damage caused by etoposide and label the sites using a DNA polymerase and fluorescently labeled nucleotides. Using this DNA-damage detection assay we find a large variation in etoposide induced DNA-damage after *in vitro* treatment of blood cells from healthy individuals. We furthermore used the TopoII inhibitor ICRF-193 to show that the etoposide-induced damage in DNA was TopoII dependent. We discuss how our results support a potential future use of the assay for personalized dosing of chemotherapy.

1. Introduction

The treatment of cancer includes DNA-damaging agents like radiation and chemotherapy [1]. Chemotherapeutic drugs, such as cisplatin, doxorubicin and etoposide, induce DNA damage of various forms, such as double-strand breaks (DSBs), single-strand breaks (SSBs), crosslinks and damaged bases [2]. DNA damage is more toxic to the rapidly dividing cancer cells [3–6], but also results in adverse side effects in fast dividing normal tissue, such as the bone marrow and the gastrointestinal tract. There is a variation in both the cancer treatment efficiency and the severity of normal tissue toxicity, due to interindividual variations in drug bioavailability, inherent individual sensitivity to DNA-damage, previous chemotherapy, age, as well as other factors [2,7–12]. Methods to measure and monitor interindividual variation in chemotherapy response are still lacking, which has resulted in a crude dosing model [13]. This in turn means that while some patients are underdosed so that there is little effect of the drug, other patients experience severe side effects. There is therefore a need for methods to personalize cancer therapy.

Topoisomerase II (TopoII) plays a pivotal role in DNA replication, transcription and chromosome segregation [14], and TopoII inhibitors are used for cancer chemotherapy. TopoII can untangle DNA, leading to the separation of intertwined chromosomes during anaphase by sequentially cleaving and relegating double-stranded DNA in an ATP-dependent manner [15]. Etoposide is a TopoII poison that inhibits the ligase function in the dimeric TopoII [14], which converts TopoII to a DNA-damaging agent, since the enzyme can cleave but not religate DNA [14]. As the dimeric TopoII has two ligase sites, most etoposide bound TopoII molecules will generate SSBs at clinically relevant concentrations. At higher levels of etoposide, DSBs are also generated as the available ligase pockets become saturated [16]. Etoposide has also been demonstrated to

Abbreviations: SSB, single-strand break; DSB, double-strand break; BER, base excision repair; PBMC, peripheral blood mononuclear cells; TopoII, topoisomerase II.

* Corresponding author.
** Corresponding author. Biology and Biological Engineering, Chalmers University of Technology, Gothenburg, Sweden.
E-mail addresses: vsingh@chalmers.se (V. Singh), fredrikw@chalmers.se (F. Westerlund).

https://doi.org/10.1016/j.bbrc.2022.01.041

produce radicals and radical-mediated DNA-damage [17,18]. The relevance of this mode of action at clinically relevant concentrations remains to be clarified. TopoII can be inhibited by another class of molecules that hinders its nuclease function by interfering with ATP binding. ICRF-193 is an example of such an inhibitor [19]. It efficiently inhibits DNA-damage by etoposide as it locks the enzyme in a "closed clamp" conformation unable to cleave DNA [19].

Quantification of DNA lesions caused by DNA damaging agents in patient cells has the potential to be an important clinical biomarker. Techniques available to quantify DNA breaks include the comet assay [20], ligation mediated PCR [21], electrochemical detection [22], enzyme-linked immunosorbent assay (ELISA) [22], and radioimmunoassay (RIA) [23]. Since specific antibodies for the detection of all types of damages are not available, highly sensitive techniques like ELISA and RIA have not yet been used in clinical settings [24,25].

Recently, a technique that combines nick translation with single-molecule imaging to quantify single-strand DNA lesions formed by different DNA damaging agents has been developed [26]. It uses a combination of DNA repair enzymes that excise the damaged DNA lesions and make the DNA ends ready for DNA polymerase 1 action. The polymerase then adds fluorescently labeled nucleotides at each damage site. This assay has been used to quantify UV, ethanol and hydrogen peroxide induced DNA damage [26–28]. We recently demonstrated that the same assay can also be used to quantify damage induced by ionizing radiation and hyperthermia [29], bleomycin [30], as well as novel metallodrugs [31].

Here, we use the assay to quantify DNA lesions induced by etoposide on peripheral blood mononuclear cells (PBMC) from healthy individuals. We observe a large interindividual variation in the amount of damage detected for the same drug dose. We also observe a significant decrease in etoposide-induced damage levels when co-incubating with ICRF-193, indicating that the method specifically measures etoposide-induced damage. This supports the idea of potential future use of the method to personalize chemotherapy dosing for patients.

2. Materials and methods

2.1. Collection of blood samples

Excess blood (EDTA tubes) from individuals with normal differential blood count were collected from the Hematology Unit at the Clinical Chemistry Laboratory at Sahlgrenska University Hospital in Gothenburg, Sweden. Gradient centrifugation using Lymphoprep (Axis-Shield PoC AS, Oslo, Norway) was used for separation of PBMC according to the manufacturer's instructions.

2.2. Drug preparation and treatment

A 50 mM stock solution of etoposide phosphate (SANTA CRUZ) was prepared in Milli-Q water and stored at -80 °C. Approximately 2.5×10^5 lymphocytes/sample, were resuspended in RPMI 1640 in a total volume of 400 μL, treated with etoposide concentrations ranging from 0.5 μM to 100 μM, and incubated on a thermal block at 37 °C for 1 h. TopoII inhibition by ICRF-193 (Sigma Aldrich) was performed by pre-incubating PBMC (2.5×10^5 lymphocytes/400 μL) with ICRF-193 (10 μM) at 37 °C for 1 h on a thermal block, followed by incubation with etoposide (10 μM) at 37 °C for 1 h.

2.3. Fluorescent labeling of the DNA damage

After the drug treatment, DNA extraction was done using GenElute-Mammalian Genomic DNA Miniprep Kit (Sigma) kit. Wide bore tips were used to minimize DNA breaks caused by pipetting. A two-step labeling of the damaged sites was performed [26,30]. The first step involved treatment of 100 ng of DNA with APE1 (2.5 U), FpG (2.5 U), Endo III (2.5 U), Endo IV (2.5 U), Endo VIII (2.5 U) and UDG (2.5 U) in 1X CutSmart Buffer (New England BioLabs (NEB)) for 1 h at 37 °C [30]. These enzymes constitute the "enzyme cocktail". The second step involved fluorescent labeling of the damage sites with 1 μM of dATP, dGTP, dCTP, 0.25 μM dTTP (Sigma Aldrich) and 0.25 μM Aminoallyl-dUTP-ATTO-647 N (Jena Bioscience) in 1X NEBuffer 2 (NEB) and DNA polymerase 1 (1.25 U) for 1 h at 20 °C. The reaction was terminated using 2.5 μL of 0.25 M EDTA (Sigma-Aldrich).

2.4. Silanization of coverslips

The silanization of standard 22 × 22 mm glass coverslips (Superior MARIENFELD Laboratory Glassware) was adapted from Wei et al. [29,32]. The coverslips were carefully put in an acetone solution consisting of 1% APTES and 1% ATMS, (v/v) to avoid lumping that can lead to irregular silanization. The silanization was performed overnight and after the completion of silanization, the coated coverslips were rinsed with acetone, Milli-Q water three times, and then dried by air purging. The air-dried coverslips could be stored for one week.

2.5. DNA staining and imaging

The fluorescently labeled DNA (7 μL/sample) was diluted in 0.5X TBE and stained with 320 nM YOYO-1 (Invitrogen) in a total volume of 50 μL. β-mercaptoethanol (2% v/v, Sigma-Aldrich) was added just before the image acquisition to minimize photobleaching. Approximately, 3.4 μL of the sample was put at the interface of an activated coverslip and a clean microscopic slide (VWR Frosted) and the extended DNA molecules were imaged with a fluorescence microscope (Zeiss Observer.Z1) using an Andor iXON Ultra EMCCD camera equipped with a Colibri 7 LED illumination system. Two appropriate band-pass excitation filters (475/40 and 640/30) and bandpass emission filters (530/50 and 690/50), for YOYO-1 and ATTO-647 N, respectively, were used. An EM gain setting of 100 and exposure times of 50 ms and 500 ms for YOYO-1 and Aminoallyl-dUTP-ATTO-647 N, respectively, were used.

2.6. Data analysis

A custom-made software was used to determine the total DNA length in pixels and count the number of colocalized ATTO-647 N sites as dots/pixel. Fluorescent labels at the ends of the DNA were not counted to exclude DNA strand breaks caused by shear and non-specific labeling by DNA polymerase 1. Two or more overlapping DNA strands were also excluded from the quantification. The software cannot distinguish two or more dots within the diffraction limit. The DNA length was converted from pixel to μm (1 pixel = 0.129 μm) using lambda-DNA (48502 bp, New England Biolab) as a size reference. We determined that 1 μm stretched DNA = ~3000 bp, and this value was used for converting dots/pixel to dots/MBp [30]. The values were then presented as dots/MBp as follows:

Damage detected (DD, dots/Mbp) = total number of sites detected per DNA length

It is important to note that the DD-value corresponds to the number of sites that DNA polymerase 1 can elongate after the cocktail of repair enzymes has made the dirty DNA ends polymerizable.

To assess the statistical significance, the experiments were performed in technical triplicates unless otherwise noted, and

differences between the groups were assessed by ANOVA analysis (Tukey's post-hoc test) (*** represents $p < 0.001$, and * represents $p < 0.05$).

3. Results

3.1. Detection of DNA damage caused by etoposide

The protocol for quantifying single-strand lesions caused by etoposide and fluorescent labeling of the damaged sites is schematically outlined in Fig. 1 A (see Methods for details) [29,30]. PBMC were isolated from blood samples of individuals with normal blood count, treated with etoposide and the DNA was extracted. The damaged DNA was treated with BER enzymes and labeled using DNA polymerase 1 and dNTPs, including the fluorescent analogue Aminoallyl-dUTP-ATTO-647 N, leading to DNA molecules where each damage site was fluorescently labeled. The sample was then stained with YOYO-1 and stretched on a silanized glass surface. Representative images from the analysis software for untreated and 10 μM etoposide treated samples are shown in Fig. 1 B, where the etoposide treated sample harbors much more fluorescently labeled damage sites than the control.

3.2. Detection of the etoposide induced DNA damage using the enzyme cocktail

To investigate the ability of the enzyme cocktail, containing APE1, FpG, Endo III, Endo IV, Endo VIII, and UDG, to detect etoposide induced DNA damage, PBMC from mixed blood were analyzed. An increase in the level of damage was detected compared to the untreated samples (Fig. 2) (Fig. S1, Supporting Information). The DNA damage increased ~5.4 and ~8.0 times at 0.5 μM and 10 μM etoposide, respectively, compared to the no enzyme control. Interestingly, DNA polymerase 1 alone did not lead to increased DNA damage levels in the presence of etoposide. As the enzyme cocktail was required to detect the etoposide-induced damage it was used for all the following experiments.

3.3. Inter-individual variation and concentration dependent response in etoposide induced DNA damage

To explore inter-individual differences in the response to etoposide, we extended the analysis to blood samples collected from 13 healthy individuals (Fig. 3 A). To compare the etoposide induced damage, we first subtracted the damage for the untreated sample (Fig. S2, Supporting Information) from the etoposide treated samples. Interestingly, there was a ~20-fold difference between the highest and lowest level of detected damage at 10 μM etoposide concentration, with some individuals showing no significant increase compared to the untreated sample. The coefficient of variation (CV) in the etoposide induced damage for the individuals assayed was 63.3%, indicating a large variation among the tested individuals.

A potential reason for the difference in response between individuals is that the etoposide concentration required to cause a significant response differs. We next investigated the response at

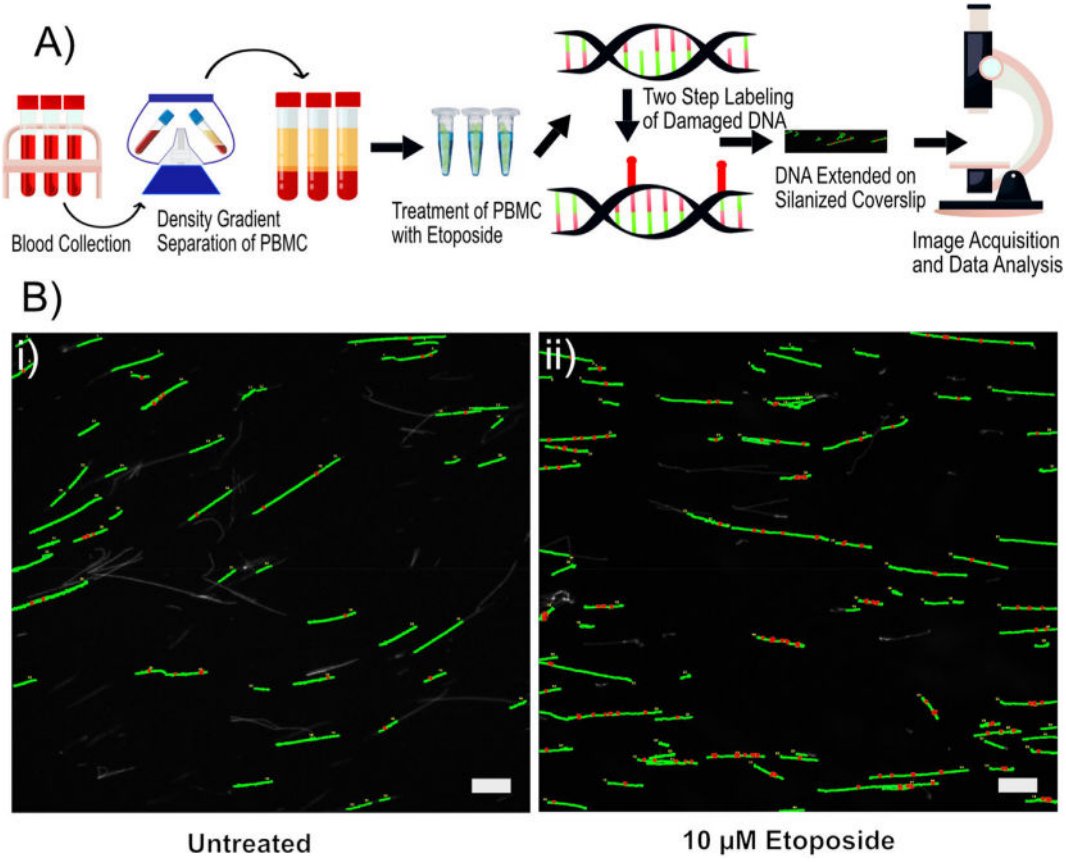

Fig. 1. (A) Schematic of the steps involved in the detection of DNA damage caused by etoposide. The labeling of etoposide induced DNA damage was performed in two steps; first the BER enzymes, collectively called the "enzyme cocktail", were used to process the damaged sites and second, these processed sites were labeled using DNA polymerase 1 and dNTPs including one fluorescent analogue. (B) Representative images from the analysis software of (i) untreated and (ii) etoposide (10 μM) treated samples. The DNA backbone was stained with YOYO-1 (green) and damage sites were labeled with Aminoallyl-dUTP-ATTO-647 N (red). Scale bar = 10 μm. (For interpretation of the references to colour in this figure legend, the reader is referred to the Web version of this article.)

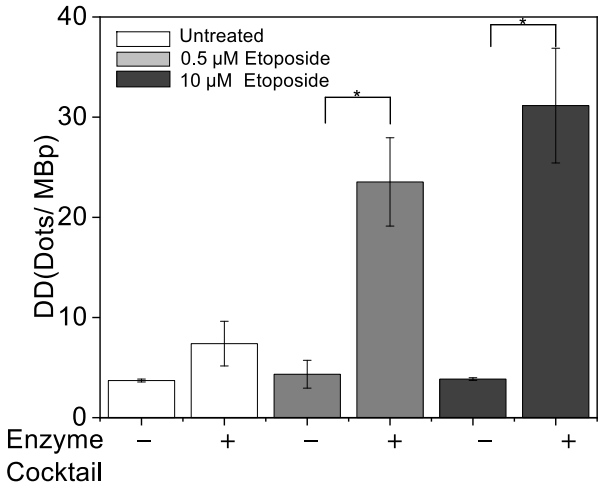

Fig. 2. DNA damage (DD-values) detected in chromosomal DNA extracted from untreated, and etoposide (0.5 μM) and (10 μM) treated, PBMC collected from pooled blood and incubated with/without enzyme cocktail. Standard deviations were calculated from independent technical duplicates.

concentrations of etoposide ranging from 0.5 μM to 100 μM for two healthy individuals (Fig. 3 B). There was a significant difference in the response of the two individuals, but for both the individuals we observed a plateau (Individual 14) and a ~28.0% decrease (Individual 15) in DD-values at the higher etoposide concentration (100 μM), respectively.

3.4. Effect of TopoII inhibition on etoposide induced DNA damage

To demonstrate that the damage detected was caused by etoposide's inhibition of TopoII, we used the TopoII inhibitor ICRF-193 (see Methods). The effect of ICRF-193 on etoposide induced strand breaks in five healthy individuals is presented in Fig. 4. ICRF-193 increased the damage detected 1.5-7.3 times without etoposide in the five individuals, indicating that ICRF-193, as expected, induces some DNA damage [19]. However, in all five individuals we observed that the damage induced by etoposide was lower (1.5-2.8 times) when ICRF-193 was present, indicating that the etoposide induced damage is mediated through inhibition of TopoII (Fig. S3, Supporting Information).

4. Discussion

Chemotherapeutic drugs can cause severe side-effects that impact the quality of life for cancer survivors or lead to mortality [33,34]. Since many such drugs induce DNA damage as their cytotoxic mechanism, methods for detecting the total amount of DNA lesions formed hold promise to be used for personalized dosing of

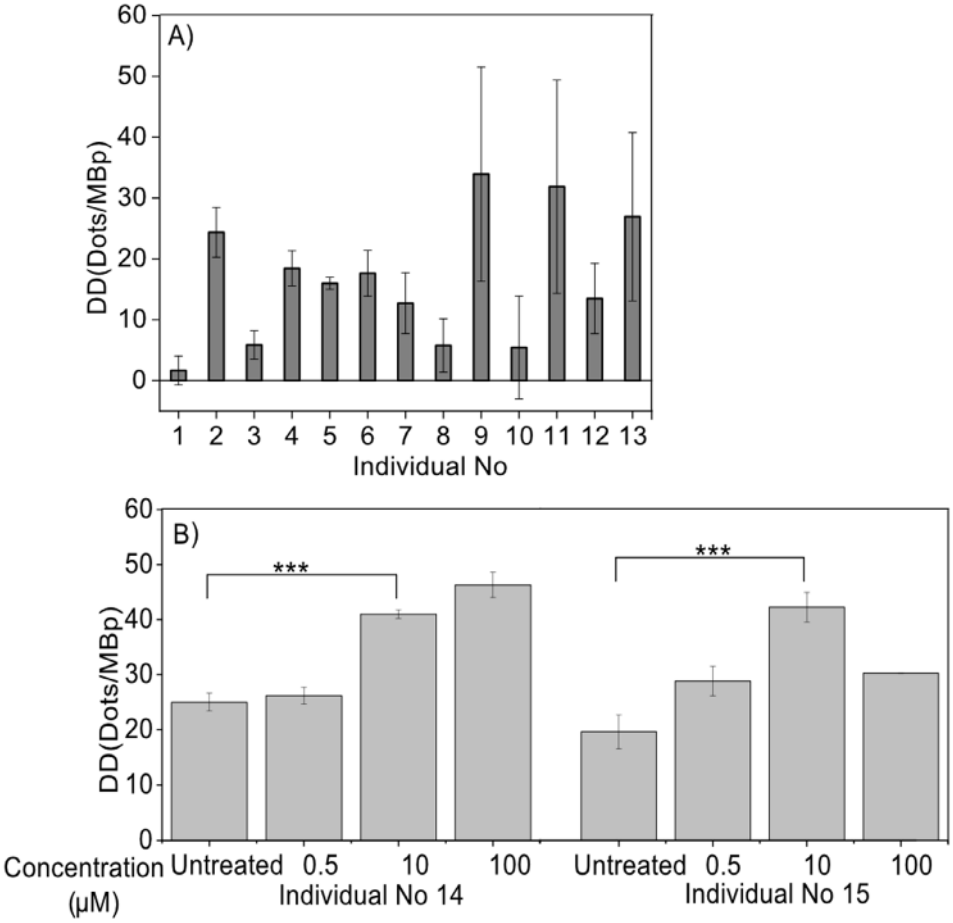

Fig. 3. (A) DNA damage (DD-values) for PBMC from thirteen healthy individuals treated with 10 μM etoposide. Standard deviations were calculated from technical duplicates (individuals 8 and 12) or technical triplicates (the other individuals). (B) DNA damage (DD-values) detected in chromosomal DNA extracted from PBMC from two healthy individuals (Individual 14 and Individual 15) exposed to increasing concentrations (from 0 to 100 μM) of etoposide. Standard deviations were calculated from technical triplicate (Individual 14) or technical duplicate (Individual 15).

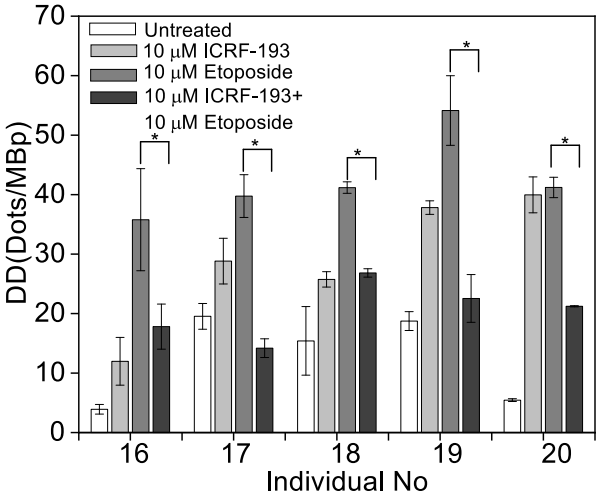

Fig. 4. DNA damage (DD-values) detected in chromosomal DNA extracted from PBMC from five healthy individuals (Individual 16-20) treated with ICRF-193 (10 μM), etoposide (10 μM), or both. Standard deviations were calculated from technical duplicates.

chemotherapy. Here, we demonstrate the use of such an assay to quantify DNA damage induced by the cytotoxic drug etoposide, a TopoII poison.

We show that the damage formed by etoposide can not be repaired by only DNA polymerase 1, but also requires the addition of a cocktail of DNA repair enzymes. This indicates that the DNA lesions formed include those that require processing by BER enzymes and are not only simple nicks that would be labeled by DNA polymerase alone. Oxidative DNA lesions, TopoII-SSB complexes and DNA protein adducts have previously been reported to be formed by etoposide treatment [35–37]. The enzyme cocktail used here was able to detect the single-strand DNA lesions at clinically relevant doses of etoposide.

A large variation between healthy individuals observed in the response to etoposide was observed. This high variation between individuals can potentially be explained by varying TopoII levels. Variations in TopoII levels have been reported widely in acute myeloid leukaemia and acute lymphoblastic leukaemia [38–40] and may be so even for normal tissue.

When titrating the concentration of etoposide we observed differences between individuals in the dose-response, in particular at high concentrations. This may be due to the saturation of TopoII poisoning at the lower concentration and/or the generation of intermediates that the enzyme cocktail cannot process completely and require additional enzymes [37,41,42] at high etoposide concentration. Therefore, special care must be taken to uncover these protein-bound DNA-breaks if one wants to measure the total extent of etoposide-induced DNA damage in patient cells [18].

We used the TopoII inhibitor ICRF-193 to demonstrate that the etoposide-induced damage detected was due to its function as a TopoII poison. ICRF-193 is known to decrease the etoposide induced strand breaks by ~50%, which agrees with our observations [43]. We also observed DNA damage caused by ICRF-193 only, which contradicts some earlier studies. We believe that we observed this activity since our cell lysis solution contains GuHCl, a chaotropic protein denaturant that is required to detect the formation of SSBs by ICRF-193 [19,44].

To conclude, we have adapted a recently developed method for detection of single-strand lesions caused by the chemotherapeutic drug etoposide. We report a large inter-patient variability in drug dose response between individuals. We also report that the DNA damage detection assay can be used to gain mechanistic insight of action of chemotherapy drugs. This assay could in the future be used both to personalize chemotherapy by determining patient sensitivity, but also to identify inhibitors and activators that can be used to design co-treatment strategies to improve future chemotherapy.

Funding

The following funding agencies are acknowledged by the authors: Swedish Cancer Foundation [2017/654 and 20 1145 PjF to F.W. and 2017/600 to O.H.], Swedish Childhood Cancer Foundation [MT2016-0004 and PR2019-0037 to F.W. and PR2020-0105 to P.J.], the Swedish Heart and Lung Foundation [to O.H.], the Assar Gabrielsson Cancer Research Foundation [to V.S. and P.J.], and LUA/ALF [to O.H.] and C4A [to P.J.] funding at Sahlgrenska University Hospital. Funding for part of the microscopy was supported by IngaBritt och Arne Lundbergs Forskningsstiftelse [to F.W.].

CRediT authorship contribution statement

Vandana Singh: Conceptualization, Methodology, Validation, Formal analysis, Investigation, Writing – original draft, Funding acquisition. **Pegah Johansson:** Conceptualization, Resources, Writing – review & editing, Supervision, Funding acquisition. **Elina Ekedahl:** Methodology. **Yii-Lih Lin:** Software. **Ola Hammarsten:** Conceptualization, Resources, Writing – review & editing, Supervision, Funding acquisition. **Fredrik Westerlund:** Conceptualization, Methodology, Writing – review & editing, Supervision, Project administration, Funding acquisition.

Declaration of competing interest

The authors declare no conflicts of interest.

Acknowledgements

The authors would like to thank the efforts of the hematology staff at the Department of Clinical Chemistry at Sahlgrenska University Hospital and Anna Lyytikäinen for providing us with blood samples. The analysis software was provided by the group of Dr. Yuval Ebenstein at Tel Aviv University. We acknowledge fruitful discussion with Dr. Yuval Ebenstein.

Appendix A. Supplementary data

Supplementary data to this article can be found online at https://doi.org/10.1016/j.bbrc.2022.01.041.

References

[1] D.S. Dizon, L. Krilov, E. Cohen, T. Gangadhar, P.A. Ganz, T.A. Hensing, S. Hunger, S.S. Krishnamurthi, A.B. Lassman, M.J. Markham, E. Mayer, M. Neuss, S.K. Pal, L.C. Richardson, R. Schilsky, G.K. Schwartz, D.R. Spriggs, M.A. Villalona-Calero, G. Villani, G. Masters, Clinical cancer advances 2016: annual report on progress against cancer from the American Society of Clinical Oncology, J. Clin. Oncol. 34 (2016) 987–1011.
[2] E. Calvo, C. Walko, E.C. Dees, B. Valenzuela, Pharmacogenomics, pharmacokinetics, and pharmacodynamics in the era of targeted therapies, Am. Soc. Clin. Oncol. Educ. Book 35 (2016) e175–e184.
[3] S. Dasari, P.B. Tchounwou, Cisplatin in cancer therapy: molecular mechanisms of action, Eur. J. Pharmacol. 740 (2014) 364–378.
[4] H. Taymaz-Nikerel, M.E. Karabekmez, S. Eraslan, B. Kırdar, Doxorubicin induces an extensive transcriptional and metabolic rewiring in yeast cells, Sci. Rep. 8 (2018) 13672.
[5] Y. Xu, C. Her, Inhibition of topoisomerase (DNA) I (TOP1): DNA damage repair and anticancer therapy, Biomolecules 5 (2015) 1652–1670.
[6] R. Rezonja, L. Knez, T. Cufer, A. Mrhar, Oral treatment with etoposide in small cell lung cancer - dilemmas and solutions, Radiol. Oncol. 47 (2013) 1–13.

[7] M.E. de Jonge, A.D. Huitema, J.H. Schellens, S. Rodenhuis, J.H. Beijnen, Individualised cancer chemotherapy: strategies and performance of prospective studies on therapeutic drug monitoring with dose adaptation: a review, Clin. Pharmacokinet. 44 (2005) 147–173.
[8] J.G. Paez, P.A. Jänne, J.C. Lee, S. Tracy, H. Greulich, S. Gabriel, P. Herman, F.J. Kaye, N. Lindeman, T.J. Boggon, K. Naoki, H. Sasaki, Y. Fujii, M.J. Eck, W.R. Sellers, B.E. Johnson, M. Meyerson, EGFR mutations in lung cancer: correlation with clinical response to gefitinib therapy, Science 304 (2004) 1497–1500.
[9] M. Malet-Martino, R. Martino, Clinical studies of three oral prodrugs of 5-fluorouracil (capecitabine, UFT, S-1): a review, Oncologist 7 (2002) 288–323.
[10] R.S. de Jong, N.H. Mulder, D.R. Uges, S. Kaul, B. Winograd, Sleijfer DTh, H.J. Groen, P.H. Willemse, W.T. van der Graaf, E.G. de Vries, Randomized comparison of etoposide pharmacokinetics after oral etoposide phosphate and oral etoposide, Br. J. Cancer 75 (1997) 1660–1666.
[11] K.R. Hande, M.G. Krozely, F.A. Greco, J.D. Hainsworth, D.H. Johnson, Bioavailability of low-dose oral etoposide, J. Clin. Oncol. 11 (1993) 374–377.
[12] H. Atamna, I. Cheung, B.N. Ames, A method for detecting abasic sites in living cells: age-dependent changes in base excision repair, Proc. Natl. Acad. Sci. U. S. A. 97 (2000) 686–691.
[13] D. Pinkel, The use of body surface area as a criterion of drug dosage in cancer chemotherapy, Cancer Res. 18 (1958) 853–856.
[14] J.L. Nitiss, Targeting DNA topoisomerase II in cancer chemotherapy, Nat. Rev. Cancer 9 (2009) 338–350.
[15] J.H. Lee, J.M. Berger, Cell cycle-dependent control and roles of DNA topoisomerase II, Genes (Basel) 10 (2019).
[16] A. Muslimović, S. Nyström, Y. Gao, O. Hammarsten, Numerical analysis of etoposide induced DNA breaks, PLoS One 4 (2009) e5859.
[17] V.E. Kagan, J.C. Yalowich, G.G. Borisenko, Y.Y. Tyurina, V.A. Tyurin, P. Thampatty, J.P. Fabisiak, Mechanism-based chemopreventive strategies against etoposide-induced acute myeloid leukemia: free radical/antioxidant approach, Mol. Pharmacol. 56 (1999) 494–506.
[18] N. Haim, J. Nemec, J. Roman, B.K. Sinha, Peroxidase-catalyzed metabolism of etoposide (VP-16-213) and covalent binding of reactive intermediates to cellular macromolecules, Cancer Res. 47 (1987) 5835–5840.
[19] K.C. Huang, H. Gao, E.F. Yamasaki, D.R. Grabowski, S. Liu, L.L. Shen, K.K. Chan, R. Ganapathi, R.M. Snapka, Topoisomerase II poisoning by ICRF-193, J. Biol. Chem. 276 (2001) 44488–44494.
[20] A.R. Collins, The comet assay for DNA damage and repair: principles, applications, and limitations, Mol. Biotechnol. 26 (2004) 249–261.
[21] C.Y. Yu, B.C. Yin, S. Wang, Z. Xu, B.C. Ye, Improved ligation-mediated PCR method coupled with T7 RNA polymerase for sensitive DNA detection, Anal. Chem. 86 (2014) 7214–7218.
[22] G. Figueroa-González, C. Pérez-Plasencia, Strategies for the evaluation of DNA damage and repair mechanisms in cancer, Oncol. Lett. 13 (2017) 3982–3988.
[23] I.J. Chopra, D.H. Solomon, G.N. Beall, Radioimmunoassay for measurement of triiodothyronine in human serum, J. Clin. Invest. 50 (1971) 2033–2041.
[24] T.R. Berton, D.L. Mitchell, Quantification of DNA photoproducts in mammalian cell DNA using radioimmunoassay, Methods Mol. Biol. 920 (2012) 177–187.
[25] M.S. Cooke, R. Olinski, S. Loft, E.S.C.o.U.D.L. Analysis, Measurement and meaning of oxidatively modified DNA lesions in urine, Cancer Epidemiol. Biomark. Prev. 17 (2008) 3–14.
[26] S. Zirkin, S. Fishman, H. Sharim, Y. Michaeli, J. Don, Y. Ebenstein, Lighting up individual DNA damage sites by in vitro repair synthesis, J. Am. Chem. Soc. 136 (2014) 7771–7776.
[27] J. Lee, H.S. Park, S. Lim, K. Jo, Visualization of UV-induced damage on single DNA molecules, Chem. Commun. (Camb) 49 (2013) 4740–4742.
[28] J. Lee, Y. Kim, S. Lim, K. Jo, Single-molecule visualization of ROS-induced DNA damage in large DNA molecules, Analyst 141 (2016) 847–852.
[29] V. Singh, P. Johansson, D. Torchinsky, Y.L. Lin, R. Öz, Y. Ebenstein, O. Hammarsten, F. Westerlund, Quantifying DNA damage induced by ionizing radiation and hyperthermia using single DNA molecule imaging, Transl. Oncol. 13 (2020) 100822.
[30] V. Singh, P. Johansson, Y.L. Lin, O. Hammarsten, F. Westerlund, Shining light on single-strand lesions caused by the chemotherapy drug bleomycin, DNA Repair (Amst) 105 (2021) 103153.
[31] N. McStay, C. Slator, V. Singh, A. Gibney, F. Westerlund, A. Kellett, Click and cut: a click chemistry approach to developing oxidative dna damaging agents, Nucl. Acids Res. (2021).
[32] Q. Wei, W. Luo, S. Chiang, T. Kappel, C. Mejia, D. Tseng, R.Y. Chan, E. Yan, H. Qi, F. Shabbir, H. Ozkan, S. Feng, A. Ozcan, Imaging and sizing of single DNA molecules on a mobile phone, ACS Nano 8 (2014) 12725–12733.
[33] S.L. Tucker, I. Turesson, H.D. Thames, Evidence for individual differences in the radiosensitivity of human skin, Eur. J. Cancer 28A (1992) 1783–1791.
[34] A. Safwat, S.M. Bentzen, I. Turesson, J.H. Hendry, Deterministic rather than stochastic factors explain most of the variation in the expression of skin telangiectasia after radiotherapy, Int. J. Radiat. Oncol. Biol. Phys. 52 (2002) 198–204.
[35] M. Tammaro, S. Liao, N. Beeharry, H. Yan, DNA double-strand breaks with 5' adducts are efficiently channeled to the DNA2-mediated resection pathway, Nucl. Acids Res. 44 (2016) 221–231.
[36] S.A. Walles, R. Zhou, E. Liliemark, DNA damage induced by etoposide; a comparison of two different methods for determination of strand breaks in DNA, Cancer Lett. 105 (1996) 153–159.
[37] Y. Kametani, C. Takahata, T. Narita, K. Tanaka, S. Iwai, I. Kuraoka, FEN1 participates in repair of the 5'-phosphotyrosyl terminus of DNA single-strand breaks, Carcinogenesis 37 (2016) 56–62.
[38] S.H. Kaufmann, J.E. Karp, P.J. Burke, S.D. Gore, Addition of etoposide to initial therapy of adult acute lymphoblastic leukemia: a combined clinical and laboratory study, Leuk. Lymphoma 23 (1996) 71–83.
[39] R. Zhou, S. Vitols, A. Gruber, J. Liliemark, Y. Wang, E. Liliemark, Etoposide-induced DNA strand breaks in relation to p-glycoprotein and topoisomerase II protein expression in leukaemic cells from patients with AML and CLL, Br. J. Haematol. 105 (1999) 420–427.
[40] S.H. Kaufmann, J.E. Karp, R.J. Jones, C.B. Miller, E. Schneider, L.A. Zwelling, K. Cowan, K. Wendel, P.J. Burke, Topoisomerase II levels and drug sensitivity in adult acute myelogenous leukemia, Blood 83 (1994) 517–530.
[41] K.C. Nitiss, M. Malik, X. He, S.W. White, J.L. Nitiss, Tyrosyl-DNA phosphodiesterase (Tdp1) participates in the repair of Top2-mediated DNA damage, Proc. Natl. Acad. Sci. U. S. A. 103 (2006) 8953–8958.
[42] J.L. Nitiss, K.C. Nitiss, Tdp2: a means to fixing the ends, PLoS Genet. 9 (2013), e1003370.
[43] H.M. Beere, C.M. Chresta, J.A. Hickman, Selective inhibition of topoisomerase II by ICRF-193 does not support a role for topoisomerase II activity in the fragmentation of chromatin during apoptosis of human leukemia cells, Mol. Pharmacol. 49 (1996) 842–851.
[44] R. Ishida, T. Miki, T. Narita, R. Yui, M. Sato, K.R. Utsumi, K. Tanabe, T. Andoh, Inhibition of intracellular topoisomerase II by antitumor bis(2,6-dioxopiperazine) derivatives: mode of cell growth inhibition distinct from that of cleavable complex-forming type inhibitors, Cancer Res. 51 (1991) 4909–4916.